Molecular Genetics and Metabolism Reports 24 (2020) 100626

Contents lists available at ScienceDirect

Molecular Genetics and Metabolism Reports

journal homepage: www.elsevier.com/locate/ymgmr

Case Report

Autopsy pathology of infantile neurovisceral ASMD (Niemann-Pick Disease type A): Clinicopathologic correlations of a case report

Beth L. Thurberg*

Department of Pathology, Sanofi Genzyme, Framingham, MA, USA

ARTICLE INFO

Keywords:
Niemann-Pick Disease type A
Acid sphingomyelinase deficiency
Sphingomyelin

ABSTRACT

Acid sphingomyelinase deficiency (ASMD; also known as Niemann-Pick Disease [NPD] A and B) is a rare lysosomal storage disease characterized by the pathological accumulation of sphingomyelin within multiple cell types throughout the body. The infantile neurovisceral (ASMD type A, also known as Niemann-Pick Disease type A) form of the disease is characterized by markedly low or absent enzyme levels resulting in both visceral and severe neurodegenerative involvement with death in early childhood. We report here the clinical course and autopsy findings in the case of a 3 year old male patient with infantile neurovisceral ASMD. A comprehensive examination of the autopsy tissue was conducted, including routine paraffin processing and staining, high resolution light microscopy and staining for sphingomyelin, and ultrastructural examination by electron microscopy. Profound sphingomyelin accumulation was present in virtually every organ and cell type. We report the clinicopathologic correlations of these findings and discuss the relevance of these results to the clinical practice of physicians following all patients with ASMD. This case represents one of the most extensive and detailed examinations of ASMD type A to date.

1. Introduction

Acid sphingomyelinase deficiency is a rare lysosomal storage disease that can present on a spectrum of clinical severity which may be due to varying levels of residual enzyme activity. In the less severe type B phenotype, the disease is apparent particularly within cells of the liver, spleen, lungs, and bone marrow, leading to hepatosplenomegaly, cirrhosis, pulmonary insufficiency, and hematologic abnormalities. There also exists an intermediate, chronic neurovisceral phenotype (ASMD type A/B, also known as Niemann-Pick disease type A/B). The more severe infantile neurovisceral (ASMD type A or Niemann-Pick Disease type A) form of the disease is characterized by profoundly low enzyme levels resulting in both visceral and severe neurodegenerative involvement with death in early childhood [1].

Opportunities to study these disorders are infrequent because of their low incidence, challenging diagnosis, and the rarity of a timely, thorough, and properly conducted metabolic autopsy. The ideal metabolic autopsy is one in which the diagnosis has been established during the patient's lifetime, and prompt collection of tissues is performed within one to 3 h of the patient's death. Consequently, when such a case arises, it presents a valuable opportunity to better understand the far-reaching potential of this disease to affect multiple organ systems. As the type A disease sits on the severe end of the spectrum of ASMD, the profound cellular and organ involvement observed here may bring to light the potential of subtle, unrecognized, or silent manifestations of the less severe type B disease.

2. Materials and methods

We received representative samples of each organ from a complete autopsy. A portion of each sample was fixed in 10% neutral buffered formalin (NBF), processed into paraffin blocks, sectioned, and stained with routine hematoxylin and eosin, or trichrome stain for fibrosis. A separate portion of each sample was fixed in 2% glutaraldehyde/2% paraformaldehyde in 0.2 M sodium cacodylate buffer, pH 7.3, and processed into epon blocks for high resolution light microscopy and electron microscopy as previously described [2]. The tissue was donated to Sanofi Genzyme for research purposes by the Wylder Nation Foundation. Both parents of the deceased provided full informed consent to the tissue donation and access to the medical record for the purpose of advancing the research of this rare disease.

* Corresponding author at: Five Mountain Road, Framingham, MA 01701-9322, USA.
E-mail address: bthurberg@gmail.com.

https://doi.org/10.1016/j.ymgmr.2020.100626
Received 3 June 2020; Received in revised form 27 June 2020

3. Results

3.1. Case history

The patient was a three year old male who was diagnosed with infantile neurovisceral ASMD (ASMD type A). The following is a chronology of the patient's clinical course.

- At birth: The infant presented with mild jaundice and dysphagia.
- Age 3 months: Signs of reflux, diarrhea, poor weight gain, anemia, and a small abdominal wall hernia became clinically apparent. An ultrasound revealed enlargement of liver and spleen. Liver enzymes were markedly elevated (Table 1).
- Age 7 months: A liver biopsy was performed. Pathology showed foamy macrophages clustered in portal regions and along sinusoids, suggestive of a lysosomal storage disorder. Subsequent enzyme and genetic testing confirmed the diagnosis of infantile neurovisceral ASMD. Acid sphingomyelinase levels were undetectable. The patient was heterozygous for a novel D253H missense change, and the c.1785_1786delTT mutation which creates a premature stop codon predicted to cause loss of normal protein function through protein truncation.
- Age 8 months: ECG testing suggested left ventricular hypertrophy. An abdominal ultrasound revealed splenomegaly and hepatic steatosis. Brain MRI showed diminished volume and myelination of white matter. Clinical development assessments revealed that the patient had not acquired any new skills since 6 months of age. Motor delay was also noted.
- Age 9 months: Clinical evaluation of the patient suggested CNS and PNS involvement of the disease. A brainstem auditory evoked potential study pointed to brainstem abnormalities. EMG evaluation suggested a demyelinating neuropathy. Liver enzymes remained markedly elevated (Table 1). The patient was assessed for possible stem cell treatment, but the family declined. Daily physical, occupational, and feeding therapy at home was initiated.
- Age 12 months: The patient continued to have feeding difficulties and at 16 months was diagnosed with chronic cholecystitis/cholelithiasis. He underwent cholecystectomy and G-tube placement.
- Age 17 months: Treatment with albuterol and Pulmacort for breathing difficulties was initiated.
- Age 19 months: The parents noticed behavioral changes. The patient was diagnosed with hydrocephalus and a VP shunt was placed.
- Age 21 months: An echocardiogram showed tricuspid and mitral valve regurgitation. Abdominal ultrasound showed diffuse fatty infiltration of the liver.
- Age 23 months: The patient exhibited increased feeding difficulty with frequent vomiting, and was placed on total parenteral nutrition (TPN). He subsequently developed severe ascites (800 cc) and underwent placement of a catheter for continuous abdominal fluid draining. The VP shunt was converted to a VA shunt.
- Age 30 months: Hypernatremia was diagnosed during a hospitalization.
- Age 35 months: Patient hospitalized and treated for pneumonia.
- Age 37 months: The patient underwent surgery to remove a growth on the right ankle, diagnosed as a hemangioma.
- Age 38 months: The patient passed away peacefully at home.

Table 1
Select laboratory values. These laboratory values were extracted from the patient's medical record to illustrate abnormalities (highlighted in grey) which may reflect some of the pathology observed at autopsy.

	3 mo	6 mo	7 mo	9 mo	Normal Ranges
RBC	3.68 L				3.80-5.40 m/mm3
Hgb	10.1 L		9.9 L		10.5-14.0 g/dL
Hct	29.4 L		27.5 L		32.0-42.0 %
Retic count	1.6% H				0.5-1.5%
Alk Phos	451 H	436 H		365 H	24-260
AST	439 H	329 H		329 H	30-120 U/L
ALT	212 H	188 H		317 H	5-45 U/L
globulin		1.2 L			2.0-3.7 g/dL
Ammonia	49 H				9-35 umol/L
Cr	0.27 L				0.40-0.70 mg/dL
GFR				90.8	85-150 ml/min/1.73m2
Total chol		153			<170 mg/dL
HDL		37 L			>39 mg/dL
LDL		97			<110 mg/dL
Trigly		112			<150 mg/dL

3.2. Clinicopathologic findings at autopsy

A detailed list of all organs examined and the specific cell types affected by sphingomyelin accumulation for each organ is shown in Table 2. Below we highlight the clinicopathologic findings for each organ system. We also note the normal (nl) organ weights for a 3-year-

Table 2
Sphingomyelin accumulation was present in cells of multiple organs. The list of affected cells reflects the availability of autopsy samples. In some organs, certain cell types could not be assessed (e.g. adrenal medulla) due to the sampling location of organ tissues made available to the author for examination.

Organ	Cells with sphingomyelin accumulation
Brain: cortex	• Neurons • Capillary endothelial cells • Vascular smooth muscle cells
Brainstem	• Neurons
Tongue	• Skeletal myocytes
Trachea	• Fibroblasts in surrounding connective tissue • Myocytes
Thyroid	• Follicular epithelial cells • Intersitial cells • Vascular endothelial cells • Vascular smooth muscle cells
Esophagus	• Endothelial cells of capillaries and lymphatics • Macrophages within the lamina propria • Smooth muscle cells of the muscularis propria
Lung	• Alveolar macrophages • Bronchiolar epithelium • Note: massive mixed inflammatory cell infiltrate present
Heart	• Cardiomyocytes • Capillary endothelial cells • Vascular smooth muscle cells • Interstitial fibroblasts
Aorta	• Vascular smooth muscle cells of the media
Small intestine	• Ganglion cells of myenteric plexus (Auerbach's) • Vascular endothelial cells • Vascular smooth muscle cells • Smooth muscle cells of the muscularis externa
Liver	• Hepatocytes • Kupffer cell within sinusoids • Clusters of foamy macrophages around portal triads
Spleen	• Splenic macrophages • Vascular endothelial cells
Lymph nodes	• Macrophages
Bone marrow	• Bone marrow cavity filled with engorged Niemann Pick cells
Pancreas	• Acinar cells of exocrine pancreas • Lower levels of sphingomyelin in endocrine pancreas islet cells
Adrenal	• All cells in all zones of the cortex • No medulla present in sample for evaluation
Kidney	• Cells of Bowman's capsule • Podocytes • Mesangial cells • Glomerular capillary endothelial cells • Proximal tubular epithelium • Interstitial capillary endothelial cells • Vascular smooth muscle cells
Skeletal muscle	• Small amounts in skeletal myocytes
Skin	• Capillary endothelial cells • Vascular smooth muscle cells

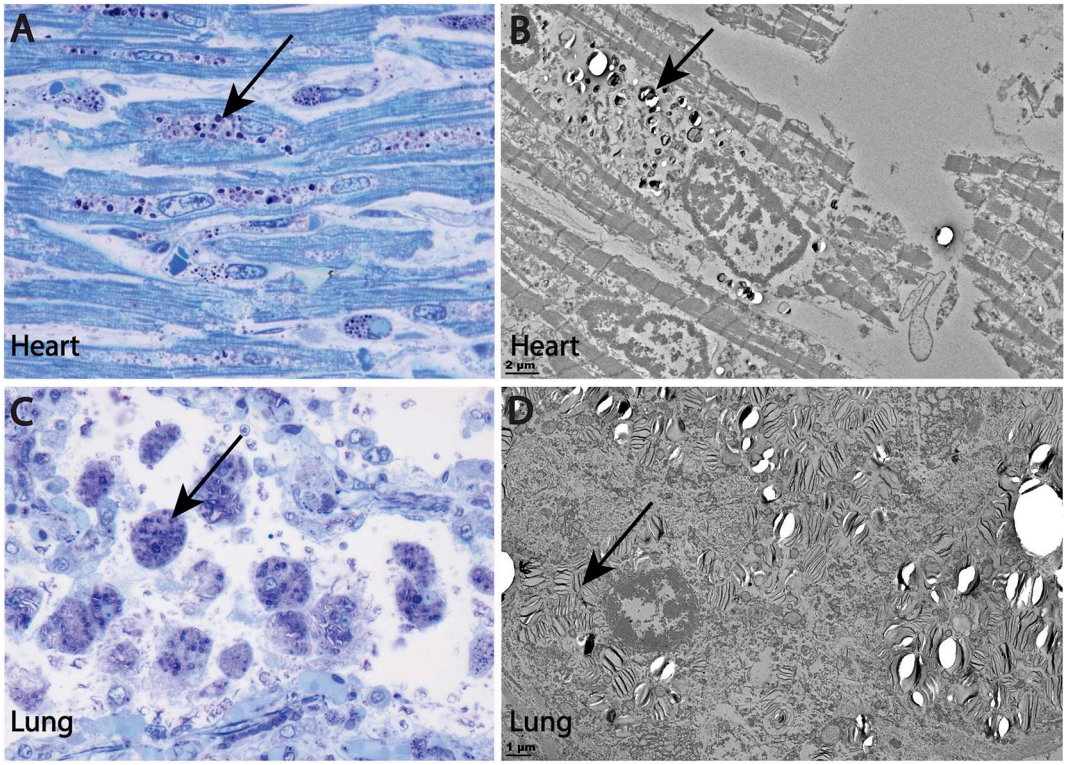

Fig. 1. Sphingomyelin accumulation was present in the heart and lungs. A. In cardiomyocytes of the left ventricular free wall, sphingomyelin appears as purple globules in high resolution microscopy sections (arrow, 1 µm epoxy resin section, modified toluidine blue stain, 1000×). B. Electron microscopy of cardiomyocytes demonstrates the "fingerprint" type whorls (arrow) characteristic of sphingomyelin accumulation in ASMD (electron microscopy, scale bar = 2 µm). C. Alveolar macrophages (arrow) of the lung are engorged with sphingomyelin, panel C. (high resolution light microscopy, 1 µm epoxy resin section, modified toluidine blue stain, 600×). D. Electron microscopy demonstrates the 'zebra body' (arrow) and 'fingerprint' architecture of the accumulated sphingomyelin within alveolar macrophages (scale bar = 1 µm).

old child [3] for comparison with abnormal organ weights noted at autopsy.

3.2.1. Cardiovascular system

Grossly, the heart was enlarged (118 g; nl = 59 g) with concentric left ventricular hypertrophy. This enlargement was likely due to the sphingomyelin accumulation observed in cardiomyocytes at the light microscopic and ultrastructural level (Fig. 1A and B, Table 2). These morphologic findings were consistent with the patient's ECG study suggestive of left ventricular hypertrophy. While we did not have the opportunity to examine the pathology of the patient's heart valves, it is worth mentioning that the tricuspid and mitral valve regurgitation observed here in the echocardiogram study at age 21 months has been observed by others reported in the ASMD literature [4], suggesting that there may be a link between the findings and disease-related substrate accumulation.

3.2.2. Pulmonary system

Both lungs weighed well above normal (right lung = 315 g, nl = 89 g; left lung = 297 g, nl = 77 g) and showed gross evidence of congestion, edema, and consolidation. These gross observations correlated with the massive infiltration of the airspaces by sphingomyelin-engorged macrophages (Fig. 1C and D; Table 2) and a mixed population of inflammatory cells, microscopically. These findings are consistent with the patient's early breathing difficulties at 17 months and later clinical pneumonia.

3.2.3. Liver and spleen

Grossly, the liver exhibited marked hepatomegaly (828 g, nl = 418 g). Portal-portal and portal-central bridging fibrosis and nodule formation on pathology (Fig. 2A) is consistent with the patient's advanced liver disease, cirrhosis, elevated liver enzymes and low globulin. Hepatocytes and Kupffer cells were engorged with sphingomyelin, which appears foamy in formalin fixed, paraffin embedded tissue sections (Fig. 2A through 2C). The patient also had low levels of HDL, a feature of the disease which has been observed in adult type B patients [5,6]. It has been hypothesized that the accumulation of sphingomyelin within the liver may contribute to dysfunction of lipoprotein metabolism and low HDL production. Reduction of sphingomyelin with enzyme replacement therapy in these adults appears to improve the low HDL levels [5,6]. The patient's gallbladder pathology was not available to us, however, the development of cholelithiasis and cholecystitis requiring cholecystectomy is not uncommon in ASMD patients [7], and is likely related to the underlying disease. The spleen was also markedly enlarged (830 g, *n* = 37 g) and filled with sphingomyelin-laden macrophages (Fig. 2D).

3.2.4. Renal

Kidney weights were above normal (right kidney = 78 g, nl = 48 g; left kidney = 90 g, nl = 49 g). Microscopically, all cells of the renal glomerulus showed marked accumulation of sphingomyelin, including capillary endothelium, mesangial cells, podocytes, and cells of Bowman's capsule. Sphingomyelin was also present within the

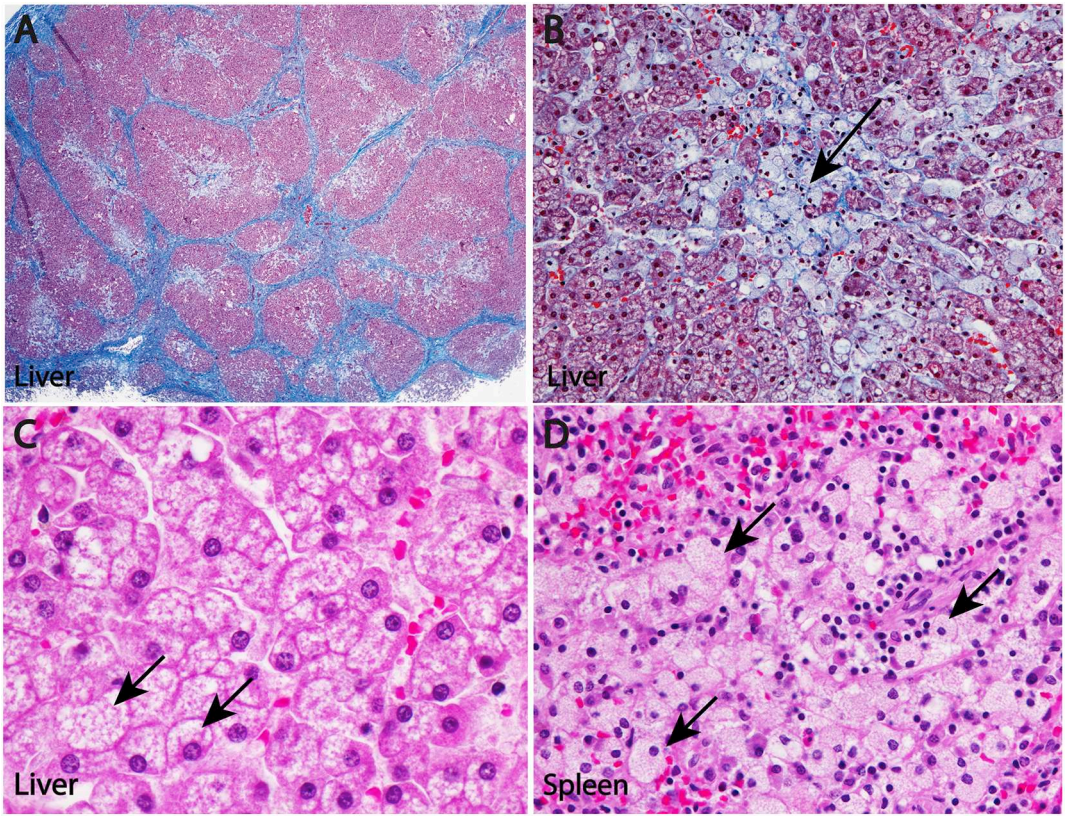

Fig. 2. Sphingomyelin accumulation was present in the liver and spleen. A. Dense portal-portal bridging bands of fibrosis (blue) appear throughout the tissue section, consistent with cirrhosis. (paraffin section, trichrome stain, 20×). B. Clusters of foamy macrophages (arrow) engorged with sphingomyelin are rimmed with pericellular fibrosis in blue (paraffin section, trichrome stain, 200×). C. At higher magnification, hepatocytes also appear foamy due to sphingomyelin accumulation (paraffin section, H & E stain, 600×). D. The spleen was also filled with foamy macrophages (paraffin section, H & E stain, 400×).

epithelial cells of proximal convoluted tubules and within vascular smooth muscle cells and endothelial cells of the interstitial vessels (Fig. 3A through 3D; Table 2). Despite the dramatic accumulation of sphingomyelin within the kidney, there was no specific evidence of renal dysfunction during the patient's clinical course. The adrenals appeared grossly normal, but microscopically, exhibited massive accumulation of sphingomyelin within all cells of the cortex. The region of the medulla was not available for examination. (Fig. 4B; Table 2).

3.2.5. Gastrointestinal system

The gastrointestinal system appeared grossly normal. Microscopically, sphingomyelin accumulation was apparent within ganglion cells (Fig. 4C; Table 2) and muscular cells of the intestine, along with cells of the exocrine pancreas (Fig. 4E; Table 2). We speculate that these cellular features of the disease may have been contributors to abnormal gastrointestinal motility and poor weight gain.

3.2.6. Bone marrow

The bone marrow cavity was filled with classical “Niemann-Pick cells”, ie, macrophages engorged with sphingomyelin (Fig. 4D), crowding out normal hematopoietic cells. This is consistent with the patient's laboratory values, showing low RBC count, hemoglobin, hematocrit and elevated reticulocyte count.

3.2.7. Nervous system

The brain appeared grossly normal, but the weight (890 g) was below that of an average 3-year-old male (1317 g). Microscopically, sphingomyelin was observed within the neurons of the cortex and brainstem (Fig. 4A; Table 2). This cellular pathology may have been a contributor to the patient's CNS clinical observations. The findings in the brainstem along with the sphingomyelin accumulation present in skeletal myocytes of the tongue and fibroblasts and myocytes around the trachea and smooth muscle cells of the muscularis propria of the esophagus are also possible contributors to the patient's dysphagia and feeding difficulties.

4. Discussion

There are very few comprehensive clinicopathologic case reports on infantile neurovisceral ASMD (ASMD type A, NPD A) in the recent literature [8,9]. Natural history studies [10] describe a pattern of disease progression, often beginning with detection of organomegaly. This is followed by neurologic, gastrointestinal, and respiratory symptoms, along with feeding difficulties, failure to thrive, irritability, and death at an average age of 27 months. The patient reported here followed a similar clinical course. Currently, there is no effective treatment for this form of the disease. The use of bone marrow transplant and stem cell transplant have been met with limited success [11]. The significant CNS pathology reported here in particular, highlights the challenge of developing a treatment capable of accessing and treating all organ compartments affected by this disease.

This post mortem study provided a valuable opportunity to better

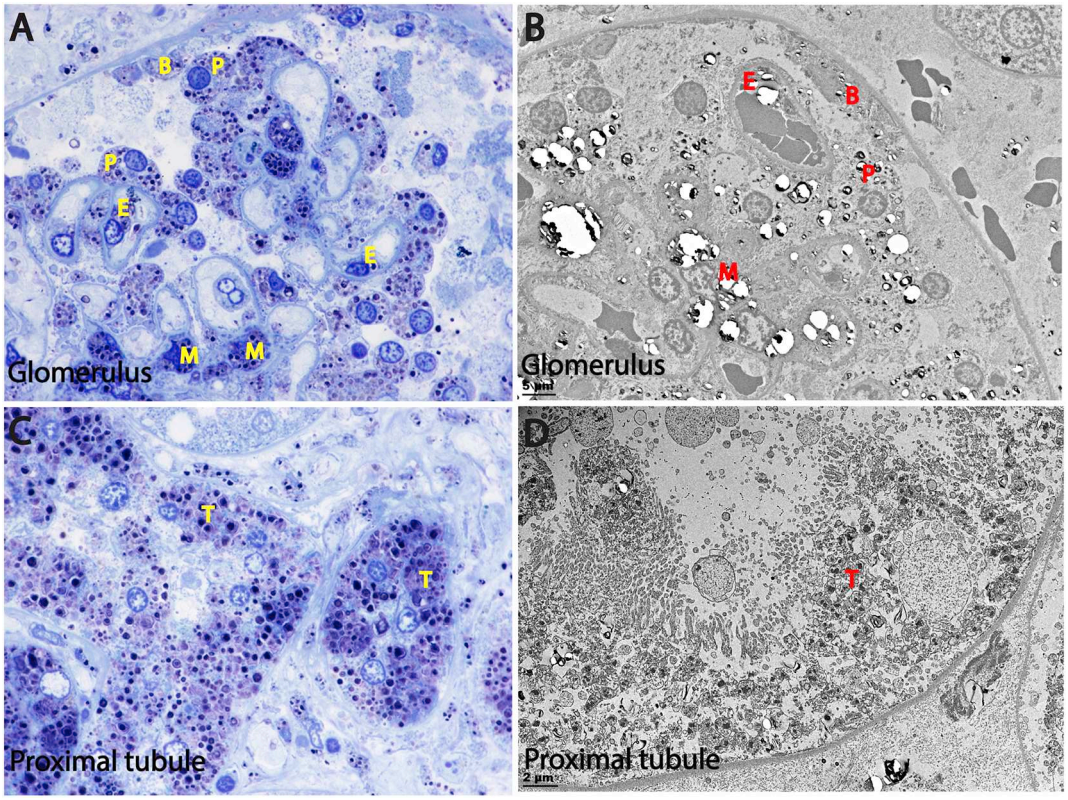

Fig. 3. Sphingomyelin is present in multiple cells types of the kidney. A. Sphingomyelin is present in numerous cell types within the renal glomerulus including podocytes (P), mesangial cells (M), capillary endothelial cells (E) and lining cells of Bowman's capsule (B) (1 µm epoxy resin section, modified toluidine blue stain, 1000×). B. Electron microscopy of the renal glomerulus illustrating the electron dense whorls of sphingomyelin within each cell type. (electron microscopy, scale bar = 5 µm). C. Sphingomyelin accumulation is also present within the epithelial cells of the proximal tubules (T) and the surrounding cells of the interstitium (1 µm epoxy resin section, modified toluidine blue stain, 1000×). D. Electron microscopy image of proximal convoluted tubule epithelium with electron dense sphingomyelin accumulation. (electron microscopy, scale bar = 2 µm). The magnitude of substrate accumulation and its specific cellular distribution is strikingly similar to the substrate accumulation observed within renal biopsies of patients with Fabry disease [14].

appreciate the profound cellular pathology of infantile neurovisceral ASMD. The complete deficiency of enzyme activity reported here, resulted in widespread cellular accumulation of sphingomyelin (Table 2) and multi-organ disease. It also serves as a reminder of the potential evolution of subclinical pathology evolving in organs of patients with the milder type B form of the disease characterized by partially deficient enzyme activity. While the classical literature on ASMD has traditionally presented the disease as a macrophage-predominant disease [12], more recent studies [5,6,13] and the present case illustrate that the enzyme deficiency is indeed global, and that all cell types throughout the body are susceptible to sphingomyelin accumulation resulting in end organ damage, similar to the widespread [14–18], and sometimes unexpected [19–24] pathology observed in other lysosomal storage disorders.

For example, the accumulation of sphingomyelin present in multiple cell types of the kidney in this patient (Fig. 3A through 3D) is as profound as that of the GL-3 accumulation observed in renal biopsies of Fabry patients [14]. In contrast to Fabry disease, physicians do not commonly associate ASMD with renal disease, and there was no specific evidence of renal dysfunction during the clinical course of our young patient. However, mild proteinuria has recently been observed as the presenting symptom in two adult female patients with ASMD. These two patients were initially referred, separately, for genetic work up with a differential diagnosis of Fabry disease in mind; however, genetic testing revealed a diagnosis of ASMD. Subsequent chest CTs revealed pulmonary infiltrates, and bone marrow biopsy revealed the presence of Niemann-Pick cells. These patients also had profoundly low HDL cholesterol levels. (Personal communication with permission, from Dr. Charles Marques Lourenço, University of Sao Paulo, Brazil). This presentation is interesting, because adult female Fabry patients commonly present with proteinuria due to the GL-3 involvement of podocytes of the renal glomerulus [14,25]. Thus, ASMD patients may present with seemingly uncommon, unrelated symptoms such as renal disease, which may in fact be due to the underlying enzyme deficiency; a mild atypical presentation not yet routinely considered in this patient population. Additional investigation of the natural history of this disease will help to determine the validity of this association.

Many of the lysosomal storage disorders present as a spectrum of disease severity. The level of residual enzyme activity is determined by the specific gene mutation, of which there are many. As a result, levels of residual enzyme activity vary from patient to patient, from near normal to absent. This variation, in turn, may correlate with the severity of pathology, clinical signs, and symptoms. When we have the opportunity to closely examine the effects of a near-complete deficiency of enzyme, we see that virtually every cell has the potential for pathologic substrate accumulation, thus leading to whole-organ dysfunction. This should bring awareness to the clinician of potentially more subtle symptoms which could be overlooked in the partially deficient patient, due to a focus on more obvious signs (eg, hepatosplenomegaly), but that nevertheless may be a consequence of the underlying disease and should be considered in the differential diagnosis of each patient.

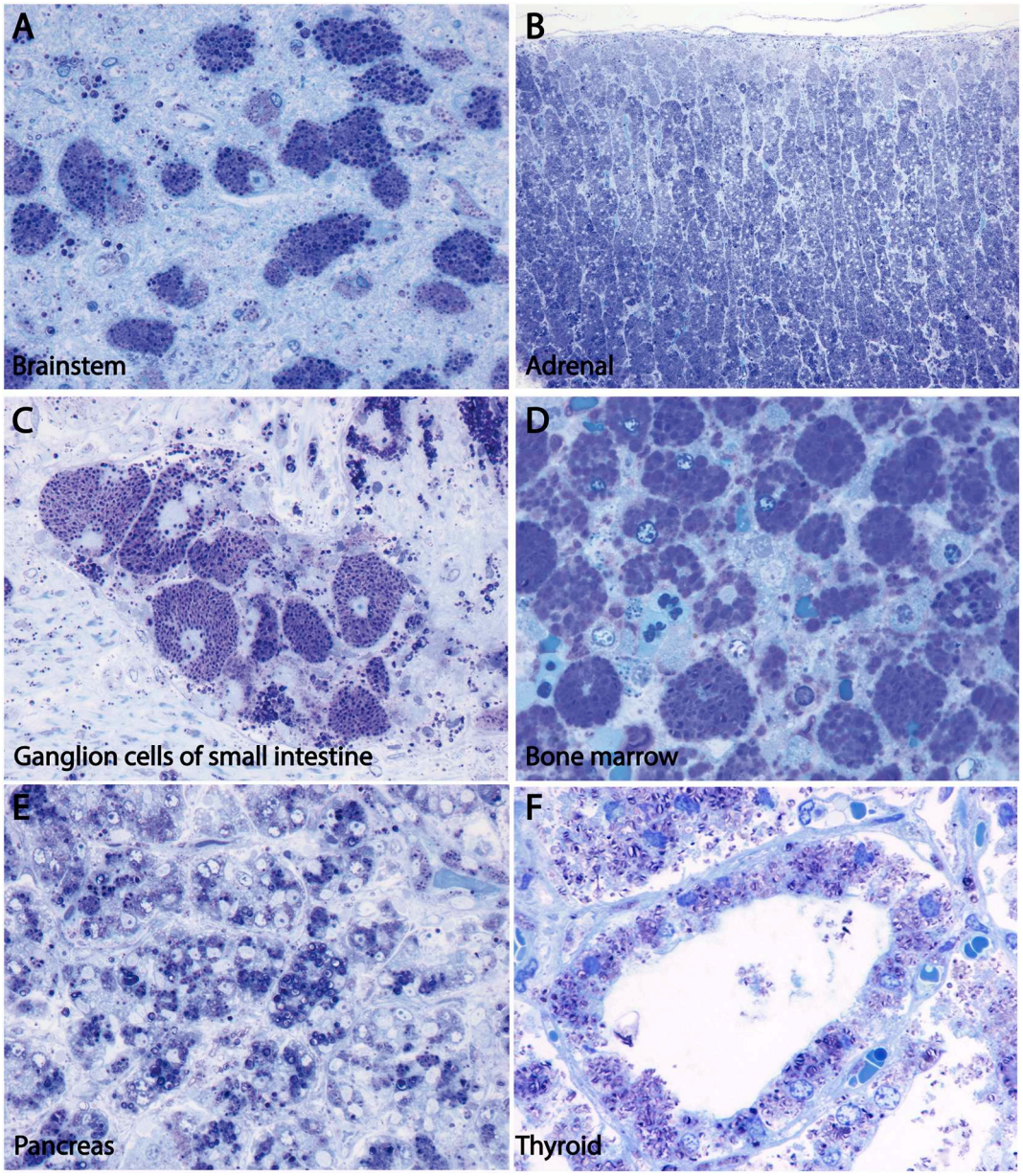

Fig. 4. Cells of multiple organs exhibited dramatic accumulation of sphingomyelin A. Neurons of the brainstem. B. Cells of the adrenal cortex. C. Ganglion cells of the small intestine. D. The bone marrow was filled with typical "Niemann-Pick' cells which crowded out the normal hematopoietic elements. E. The cells of the exocrine pancreas are also heavily laden with accumulated substrate. F. Sphingomyelin accumulation is pronounced within the follicular cells of the thyroid, as well as within the interstitial cells and vascular cells between follicles. (High resolution light microscopy, 1 μm epoxy resin sections, modified toluidine blue stain, magnifications 600×, 100×, 600×, 1000×, 600×, and 1000×, respectively).

Disclosures

Dr. Thurberg is an employee of Sanofi Genzyme.

Funding

This research did not receive any specific grant from funding agencies in the public, commercial or not-for-profit sectors.

Acknowledgments

We would like to thank the Wylder Nation Foundation for their generous tissue donation for this research. We also thank the members of the Sanofi Genzyme Department of Pathology for their expertise in lysosomal disease pathology.

References

[1] E.H. Schuchman, R.J. Desnick, Niemann-Pick Disease types A and B: Acid sphingomyelinase deficiencies, in: D. Valle, A. Beaudet, B. Vogelstein, K. Kinzler, S. Antonarakis, A. Ballabio, K. Gibson, G. Mitchell (Eds.), OMMBID-The Online Metabolic and Molecular Bases of Inherited Disease, McGraw Hill, New York, 2013, http://ommbid.mhmedical.com/content.aspx?bookid=474&Sectionid=45374145 Accessed May 2015.

[2] T.V. Taksir, J. Johnson, C.L. Maloney, E. Yandl, D. Griffiths, B.L. Thurberg, S. Ryan, Optimization of a histopathological biomarker for sphingomyelin accumulation in Niemann-Pick B Disease, J. Histochem. Biochem. 60 (8) (2012. Aug) 620–629.

[3] E. Gilbert-Barness, D.E. Debich-Spicer, Handbook of Pediatric Autopsy Pathology, Humana Press, Totowa, New Jersey, 2005 (57 and 61).

[4] I. Panigrahi, M. Dhanorkar, R. Suthar, C. Kumar, M. Baalaaji, B.R. Thapa, J. Kalra, Niemann-Pick disease: an underdiagnosed lysosomal storage disorder, Case Rep. Genet. (2019) 1–5.

[5] B.L. Thurberg, M.P. Wasserstein, S. Jones, T. Schiano, G.F. Cox, A.C. Puga, Clearance of hepatic sphingomyelin by olipudase alfa is associated with improvement in lipid profiles in acid sphingomyelinase deficiency, Am. J. Surg. Pathol. 40

(9) (2016 Sep) 1232–1242.
[6] B.L. Thurberg, G.A. Diaz, R.H. Lachmann, T. Schiano, M.P. Wasserstein, A.J. Ji, A. Zaher, M.J. Peterschmitt, Long-term olipudase alfa treatment clears hepatic sphingomyelin and improves lipoprotein profiles of patients with acid sphingomyelinase deficiency, Mol. Genet. Metab. (June 2020), https://doi.org/10.1016/j.ymgme.2020.06.010 in press.
[7] M.M. McGovern, N. Lippa, E. Bagiella, E.H. Schuchman, R.J. Desnick, M.P. Wasserstein, Morbidity and mortality in type B Niemann-Pick disease, Genet. Med. 15 (2013) 618–623.
[8] J.A. Lowden, M.S. LaRamee, P. Wentworth, The subacute form of Niemann-Pick disease, Arch. Neurol. 17 (1967) 230–237.
[9] K. Kawai, H. Hideo, T. Kimiko, An autopsy case of Niemann-Pick disease, Acta Path. Jap. 23 (4) (1973) 837–846.
[10] M.M. McGovern, A. Aron, S.E. Brodie, R.J. Desnick, M.P. Wasserstein, Natural history of Type A Niemann-Pick disease, Neurology 66 (2006) 228–232.
[11] E. Bayever, N. Kamani, P. Ferreira, G.A. Machin, M. Yudkoff, K. Conard, M. Palmieri, J. Radcliffe, D.A. Wenger, C.S. August, Bone marrow transplantation for Niemann-Pick type 1A disease, J. Inherit. Metab. Dis. 15 (1992) 919–928.
[12] C. Putterman, J. Zelingher, D. Shouval, Liver failure and the sea-blue histiocyte/adult Niemann-Pick disease, J. Clin. Gastroenterol. 15 (2) (1992) 146–149.
[13] B.L. Thurberg, M.P. Wasserstein, T. Schiano, F. O'Brien, S. Richards, G.F. Cox, M.M. McGovern, Liver and skin histopathology in adults with acid sphingomyelinase deficiency (Niemann-Pick Disease Type B), Am. J. Surg. Pathol. 36 (8) (2012 Aug) 1234–1246.
[14] B.L. Thurberg, H. Rennke, R.B. Colvin, S. Dikman, R.E. Gordon, A.B. Collins, R.J. Desnick, M. O'Callaghan, Globotriaosylceramide accumulation in the fabry kidney is cleared from multiple cell types after enzyme replacement therapy, Kidney Int. 62 (2002) 1933–1946.
[15] B.L. Thurberg, H.R. Byers, S.R. Granter, R.G. Phelps, R.E. Gordon, M. O'Callaghan, Monitoring the three year efficacy of enzyme replacement therapy in Fabry disease by repeated skin biopsies, J. Invest. Dermatol. 122 (4) (2004) 900–908.
[16] B.L. Thurberg, J.T. Fallon, R. Mitchell, T. Aretz, R.E. Gordon, M. O'Callaghan, Cardiac microvascular pathology in Fabry disease: evaluation of endomyocardial biopsies before and after enzyme replacement therapy, Circulation 118 (2009) 2561–2567.
[17] B.L. Thurberg, C. Lynch Maloney, C. Vaccaro, K. Afonso, A. Chun-Hui Tsai, E. Bossen, P.S. Kishnani, M. O'Callaghan, Characterization of pre- and post-treatment pathology after enzyme replacement for pompe disease, Lab. Investig. 86 (12) (2006 Dec) 1208–1220.
[18] Beth L. Thurberg, "Lysosomopathies: Pathophysiology and treatment of lysosomal storage diseases" chapter 7, in: E.C. Friedberg, D.H. Castrillon, R.L. Galindo, K.A. Wharton (Eds.), New-opathies: An Emerging Molecular Reclassification of Human Disease, World Scientific Publishing Company, London, 2012, pp. 231–265.
[19] J. Politei, B.L. Thurberg, E. Wallace, D. Warnock, G. Serebrinsky, C. Durand, A.B. Schenone, Gastrointestinal involvement in Fabry disease. So important, yet often neglected, Clin. Genet. 89 (1) (2016 Jan) 5–9.
[20] J.M. Politei, C. Durand, A.B. Schenone, A. Torres, J. Mukdsi, B.L. Thurberg, Chronic intestinal pseudo-obstruction. Did you search for lysosomal storage diseases? Mol. Genet. Metab. Rep. 11 (2017 March) 8–11.
[21] B.L. Thurberg, J.M. Politei, Histological abnormalities of placental tissues in Fabry disease: a case report and review of the literature, Hum. Pathol. 43 (4) (2012 Apr) 610–614.
[22] B.L. Thurberg, D. Germain, F. Perretta, K. Benistan, J.M. Politei, Fabry disease: four case reports of meningioma and a review of the literature on other malignancies, Mol. Genet. Metab. Rep. 11 (2016 Oct 1) 75–80.
[23] A.H. El-Gharbawy, G. Bhat, J.E. Murillo, B.L. Thurberg, C. Kampmann, K.E. Mengel, P.S. Kishnani, Expanding the clinical spectrum of late-onset Pompe disease: dilated arteriopathy involving the thoracic aorta, a novel vascular phenotype uncovered, Mol. Genet. Metab. 103 (4) (2011 Aug) 362–366.
[24] Y.H. Chien, N.C. Lee, Y.J. Tsai, B.L. Thurberg, F.J. Tsai, W.L. Hwu, Prominent vacuolation of the eyelid levator muscle in an early-treated child with infantile-onset Pompe disease, Muscle Nerve 50 (2) (2014 Aug) 301–302.
[25] A. Ortiz, J.P. Oliveira, S. Waldek, D.G. Warnock, B. Cianciaruso, C. Wanner, Nephropathy in males and females with Fabry disease: cross-sectional description of patients before treatment with enzyme replacement therapy, Nephrol. Dial. Transplant. 23 (2008) 1600–1607.